0022-3565/11/3383-879–889$25.00
THE JOURNAL OF PHARMACOLOGY AND EXPERIMENTAL THERAPEUTICS
Copyright © 2011 by The American Society for Pharmacology and Experimental Therapeutics
JPET 338:879–889, 2011

Vol. 338, No. 3
181552/3707519
Printed in U.S.A.

Characterization of a Sphingosine 1-Phosphate Receptor Antagonist Prodrug[S]

Perry C. Kennedy, Ran Zhu,[1] Tao Huang, Jose L. Tomsig, Thomas P. Mathews,[2] Marion David, Olivier Peyruchaud, Timothy L. Macdonald, and Kevin R. Lynch

Departments of Pharmacology (P.C.K., J.L.T., K.R.L.) and Chemistry (R.Z., T.H., T.P.M., T.L.M.), University of Virginia, Charlottesville, Virginia; and Institut National de la Santé et de la Recherche Médicale, Unité Mixte de Recherche 1033, Université de Lyon, Lyon, France (M.D., O.P.)

Received March 13, 2011; accepted May 31, 2011

ABSTRACT

Sphingosine 1-phosphate (S1P) is a phospholipid that binds to a set of G protein-coupled receptors ($S1P_1$–$S1P_5$) to initiate an array of signaling cascades that affect cell survival, differentiation, proliferation, and migration. On a larger physiological scale, the effects of S1P on immune cell trafficking, vascular barrier integrity, angiogenesis, and heart rate have also been observed. An impetus for the characterization of S1P-initiated signaling effects came with the discovery that FTY720 [fingolimod; 2-amino-2-(2-[4-octylphenyl]ethyl)-1,3-propanediol] modulates the immune system by acting as an agonist at $S1P_1$. In the course of structure-activity relationship studies to better understand the functional chemical space around FTY720, we discovered conformationally constrained FTY720 analogs that behave as S1P receptor type-selective antagonists. Here, we present a pharmacological profile of a lead $S1P_{1/3}$ antagonist prodrug, 1-(hydroxymethyl)-3-(3-octylphenyl)cyclobutane (VPC03090). VPC03090 is phosphorylated by sphingosine kinase 2 to form the competitive antagonist species 3-(3-octylphenyl)-1-(phosphonooxymethyl)cyclobutane (VPC03090-P) as observed in guanosine 5′-*O*-(3-[^{35}S]thio)triphosphate binding assays, with effects on downstream S1P receptor signaling confirmed by Western blot and calcium mobilization assays. Oral dosing of VPC03090 results in an approximate 1:1 phosphorylated/alcohol species ratio with a half-life of 30 h in mice. Because aberrant S1P signaling has been implicated in carcinogenesis, we applied VPC03090 in an immunocompetent mouse mammary cancer model to assess its antineoplastic potential. Treatment with VPC03090 significantly inhibited the growth of 4T1 primary tumors in mice. This result calls to attention the value of S1P receptor antagonists as not only research tools but also potential therapeutic agents.

Introduction

Sphingosine 1-phosphate (S1P) is a pleiotropic lipid signaling mediator that initiates a variety of downstream signaling cascades through its binding and activation of five G protein-coupled receptors ($S1P_1$–$S1P_5$) (Anliker and Chun, 2004). At the cellular level, S1P signaling increases survival, growth, proliferation, intracellular Ca^{2+} concentration, and rearrangement of the actin cytoskeleton (Pyne and Pyne, 2000; Ishii et al., 2004; Sanchez and Hla, 2004). Knowledge of the in vivo physiological effects of S1P signaling came to the forefront through the discovery and use of FTY720 [fingoli-

This work was supported by the National Institutes of Health National Institute of General Medical Sciences [Grants R01-GM067958 (to K.R.L. and T.L.M.), T32-GM008715 (to P.C.K.)]; an Abbott Laboratories research contract grant (to K.R.L.); and the Institut National de la Santé et de la Recherche Médicale and Comité Départemental de la Loire de la Ligue Nationale Contre le Cancer (M.D. and O.P.).

[1] Current affiliation: Anichem, North Brunswick, New Jersey.

[2] Current affiliation: The Scripps Research Institute, La Jolla, California.

Article, publication date, and citation information can be found at http://jpet.aspetjournals.org.
doi:10.1124/jpet.111.181552.

[S] The online version of this article (available at http://jpet.aspetjournals.org) contains supplemental material.

ABBREVIATIONS: S1P, sphingosine 1-phosphate; $hS1P_1$, human $S1P_1$; $mS1P_1$, mouse $S1P_1$; FTY720 (fingolimod), 2-amino-2-(2-[4-octylphenyl]ethyl)-1,3-propanediol; FTY720-P, 2-amino-2[2-(4-octylphenyl)ethyl]-1,3-propanediol,mono dihydrogen phosphate ester; VPC03090, 1-(hydroxymethyl)-3-(3-octylphenyl)cyclobutane; VPC03090-P, 3-(3-octylphenyl)-1-(phosphonooxymethyl)cyclobutane; GTP[γ-^{35}S], guanosine 5′-*O*-(3-[^{35}S]thio)triphosphate; SEW2871, 5-[4-phenyl-5-(trifluoromethyl)-2-thienyl]-3-[3-(trifluoromethyl)phenyl]-1,2,4-oxadiazole; VPC23019, (*R*)-phosphoric acid mono-[2-amino-2-(3-octyl-phenylcarbamoyl)-ethyl] ester; VPC44116, (*R*)-3-amino-(3-octylphenylamino)-4-oxobutylphosphonic acid; W146, (*R*)-3-amino-(3-hexylphenylamino)-4-oxobutylphosphonic acid; CHO, Chinese hamster ovary; GFP, green fluorescent protein; S1[^{33}P], ^{33}P-labeled sphingosine 1-phosphate; CHAPS, 3-[(3-cholamidopropyl)dimethylammonio]-1-propanesulfonic acid; ERK, extracellular signal-regulated kinase; VPC03099, 1-(hydroxymethyl)-3-(3-nonaphenyl)cyclobutane; VPC03093, 3-(3-heptylphenyl)-1-(phosphonooxymethyl)cyclobutane; LC-MS, liquid chromatography-mass spectrometry; E_{max}, maximal efficacy; LPA, lysophosphatidic acid; VPC01091, 1-[1-amino-3-(4-octylphenyl)cyclopentyl]methanol; ANOVA, analysis of variance; TV, tumor volume; SAR, structure-activity relationship; PBS, phosphate-buffered saline.

mod; 2-amino-2-(2-[4-octylphenyl]ethyl)-1,3-propanediol], an $S1P_{1/3/4/5}$ receptor agonist prodrug that induces lymphopenia in mice and prolongs the survival of skin transplant allografts (Chiba et al., 1996; Kiuchi et al., 2000; Brinkmann et al., 2002; Mandala et al., 2002; Kihara and Igarashi, 2008). It is now appreciated that S1P receptor stimuli contribute to the modulation of immune cell trafficking, angiogenesis, and heart rate (Spiegel and Milstien, 2003; Hait et al., 2006; Brinkmann, 2007). FTY720 established the value of S1P receptor compounds as not only research tools, but also potential therapeutic agents, given that FTY720 is now a United States Food and Drug Administration-approved drug (Gilenya) for multiple sclerosis (Brinkmann et al., 2010), and other $S1P_1$ agonists have already been evaluated in clinical trials (Cusack and Stoffel, 2010). Studies have mapped lymphopenia and bradycardia in rodents onto the $S1P_1$ and $S1P_3$ receptors, respectively. For example, a selective $S1P_1$ agonist (5-[4-phenyl-5-(trifluoromethyl)-2-thienyl]-3-[3-(trifluoromethyl) phenyl]-1,2,4-oxadiazole; SEW2871) induces lymphopenia (but not bradycardia) in wild-type mice, whereas FTY720 or its phosphorylated analogs fail to produce bradycardia in $S1P_3$ knockout mice [*S1pr3*(−/−)] (Forrest et al., 2004; Sanna et al., 2004). These findings provide an impetus to discover more selective compounds that would have greater utility in the elucidation of S1P signaling and potential clinical use.

In addition to receptor-selective agonists such as SEW2871, competitive S1P receptor antagonists have provided insight into the physiological effects of S1P signaling, particularly involving $S1P_1$. (*R*)-3-amino-(3-octylphenylamino)-4-oxobutylphosphonic acid (VPC44116) ($S1P_{1/3}$ antagonist) and an analog, (*R*)-3-amino-(3-hexylphenylamino)-4-oxobutylphosphonic acid (W146) ($S1P_1$ antagonist), both were found to increase capillary permeability as measured by Evans blue dye leakage in mouse lung tissue (Sanna et al., 2006; Foss et al., 2007). It is noteworthy that 2-amino-2[2-(4-octylphenyl)ethyl]-1,3-propanediol, mono dihydrogen phosphate ester (FTY720-P) has been proposed as a superagonist that acts as a functional antagonist to down-regulate $S1P_1$ and inhibit both tumor growth and tumor angiogenesis (LaMontagne et al., 2006). In vivo use of $S1P_1$-selective small interfering RNA also reduces tumor volume and tumor angiogenesis in mice, further supporting a potential pathological role of $S1P_1$ in cancer progression (Chae et al., 2004). Several reports have implicated S1P in cancer development (Xia et al., 2000; Akao et al., 2006; Oskouian et al., 2006; Visentin et al., 2006; Pyne and Pyne, 2010; Watson et al., 2010). It has been suggested that an inhibitor of S1P signaling, for example, an $S1P_1$ receptor antagonist, might have a beneficial dual mode of action by inhibiting hyperproliferative signaling at the cancer cells and angiogenesis at the endothelial cells (Sabbadini, 2006). However, such antagonist compounds are scarce, and the pharmacokinetic profiles of the few available have precluded their use in animal models of disease.

We explored the functional chemical space of FTY720 through structure-activity relationship (SAR) studies and discovered a conformationally constrained analog that combines the desirable pharmacokinetic properties of FTY720 with S1P receptor subtype-specific antagonism. Herein we profile this competitive $S1P_{1/3}$ antagonist prodrug, 1-(hydroxymethyl)-3-(3-octylphenyl)cyclobutane (VPC03090). We further assessed lymphopenia and vascular leakage in mice as in vivo physiological indicators of S1P receptor modulation and the ability of VPC03090 to inhibit tumor growth in an immunocompetent mouse mammary cancer model. Although VPC03090 treatment produced no changes in peripheral lymphocyte counts or vascular permeability in mice, it did inhibit the growth of 4T1 syngeneic mouse mammary tumors. Our findings underscore the importance of S1P antagonists as both research tools and aids to the development of new therapeutic scaffolds and drugs.

Materials and Methods

Materials. Chinese hamster ovary (CHO) cells were obtained from the American Type Culture Collection (Manassas, VA). Geneticin (G418 sulfate) and GDP were from Thermo Fisher Scientific (Waltham, MA). Cell culture materials were from Invitrogen (Carlsbad, CA). Charcoal/dextran-stripped fetal bovine serum was purchased from Gemini Bio-Products (Woodland, CA). Sodium orthovanadate, saponin, probenecid, and fatty acid-free bovine serum albumin were from Sigma-Aldrich (St. Louis, MO). S1[^{33}P], GTP[γ-^{35}S], and 96-well GF/C filter plates were purchased from Perkin-Elmer Life and Analytical Sciences (Waltham, MA). S1P was from Avanti Polar Lipids (Alabaster, AL). Fluo-4AM Ca^{2+} fluorophore was from Invitrogen. SEW2871 was from Cayman Chemical (Ann Arbor, MI).

Animals. C57BL/6j mice were obtained from The Jackson Laboratory (Bar Harbor, Maine) and handled in compliance with the National Institutes of Health *Guide for the Care and Use of Laboratory Animals* (Institute of Laboratory Animal Resources, 1996). $S1P_4$ null mice, in which the $S1P_4$ coding exon was replaced by a neomycin selection marker gene cassette, were made under contract with Ingenious Targeting Laboratories (Stony Brook, NY). Embryonic stem cells used to generate these mice were hybrids of both the C57BL/6 and SV129 genetic backgrounds. $S1P_4$ heterozygote mice were crossed to yield homozygote $S1P_4$ null offspring. These mice are viable and fertile. All procedures were preapproved by the Institutional Animal Care and Use Committee of the University of Virginia. Mice used in the 4T1 mammary cancer model were handled according to the rules of Décret 87-848 of Oct. 19, 1987, Paris. This experimental protocol was reviewed and approved by the Institutional Animal Care and Use Committee of the Université Claude Bernard Lyon-1 (Lyon, France). BALB/c mice, 6 weeks of age, were housed under barrier conditions in laminar flow isolated hoods. Autoclaved water and mouse chow were provided ad libitum. Animals bearing tumors were carefully monitored for signs of distress and were humanely euthanized when distress was observed.

Stable Expression of S1P Receptors in CHO Cells. pcDNA3.1+ plasmids containing the DNA sequences for each human sphingosine 1-phosphate receptor ($S1P_2$-$S1P_5$) were obtained from the University of Missouri (Rolla, MO). These plasmids, encoding the amino-terminal triple hemagglutinin-tagged forms of the S1P receptors, as well as ampicillin and neomycin/geneticin resistance, were transfected into CHO cells using Lipofectamine 2000 (Invitrogen). Cells expressing the desired S1P receptor were selected by fluorescence-activated cell sorting in a 96-well format using anti-hemagglutinin-phycoerythrin fluorescent antibody (Miltenyi Biotec, Inc., Auburn, CA) and a FACSVantage SE Turbo Sorter (BD Biosciences, Franklin Lakes, NJ). A similar plasmid encoding a GFP-tagged human $S1P_1$ receptor was used to transfect CHO cells that were then sorted based on GFP fluorescence. Expression of the mouse $S1P_1$ receptor was achieved by stable transfection of CHO cells using a plasmid containing the mouse $S1P_1$ expression sequence with an amino-terminal epitope Flag tag in a pcDNA3 vector, followed by similar fluorescence-activated cell sorting using a conjugated anti-Flag fluorescent antibody (Sigma-Aldrich). Isolated clonal populations for each receptor type were maintained under selection by incorporation of 1 mg/ml geneticin (G418) into Ham's F12 media containing 10% charcoal/dextran-stripped fetal bovine serum, 1% sodium pyruvate, and 1% penicillin and streptomycin solution. Cells were grown at 37°C in a 5% CO_2/95% air atmosphere.

GTP[γ-^{35}S] Binding Assay. Membranes prepared from CHO cells stably expressing S1P receptors were incubated in 96-well plates in 100 μl of binding buffer (50 mM HEPES, 10 mM $MgCl_2$, and 100 mM NaCl, pH 7.5, containing 0.1% fatty acid-free bovine serum albumin) with 5 μg of saponin, 11.5 μM GDP, 0.3 nM [γ-^{35}S]GTP (1200 Ci/mmol), and a range of S1P or 3-(3-octylphenyl)-1-(phosphonooxymethyl)cyclobutane (VPC03090-P) concentrations for 30 min at 30°C. Membranes were recovered on GF/C filter plates using a 96-well Brandel Cell Harvester (Brandel Inc., Gaithersburg, MD), and these plates were analyzed for bound radionuclide using a TopCount beta scintillation counter (PerkinElmer Life and Analytical Sciences).

S1[^{33}P] Radioligand Binding Assay. CHO cells stably expressing recombinant S1P receptor types were incubated in 96-well plates in 240 μl of binding buffer (50 mM HEPES, 10 mM $MgCl_2$, and 100 mM NaCl, pH 7.5, containing 0.4% fatty acid-free bovine serum albumin and 1 mM sodium orthovanadate) with various VPC03090-P or S1P concentrations, and 20 pM S1[^{33}P] (3000 Ci/mmol) for 1 h at 4°C. Cells were isolated on GF/C filter plates using a 96-well Brandel Cell Harvester, and filter plates containing cells were analyzed for bound radionuclide using a TopCount beta scintillation counter (PerkinElmer Life and Analytical Sciences). Background subtraction was performed before software analysis of binding curves.

Determination of the Binding Affinity (K_i or K_d) of VPC03090-P for the S1P Receptors. Data from the GTP[γ-^{35}S] binding assay were analyzed using a sigmoidal dose-response nonlinear regression model in Prism software (GraphPad Software, Inc., San Diego, CA) to produce EC_{50} values. Dose ratios were calculated as the ratio between the EC_{50} values for agonist in the presence and absence of antagonist VPC03090-P. Schild regression analysis was performed by plotting log (dose ratio − 1) versus log antagonist concentration and finding the K_i value from the antilog of the x-intercept of the line of best fit. S1[^{33}P] radioligand binding curve data were analyzed by nonlinear regression in Prism software to ascertain IC_{50} values. K_i (or K_d for VPC03090-P as agonist) values were determined from IC_{50} values using the Cheng-Prusoff equation: $K_i = IC_{50}/[1 + (\text{radioligand concentration/affinity of radioligand for receptor})]$, where the radioligand concentration of S1[^{33}P] was 20 pM (Cheng and Prusoff, 1973).

Western Blotting. CHO cells stably transfected to express recombinant human $S1P_1$ were cultured and grown to confluence on 100-mm plates in Ham's F12 media containing 10% charcoal/dextran-stripped fetal bovine serum, 1% sodium pyruvate, 1% penicillin and streptomycin solution, and 1 mg/ml geneticin. The cells were then serum-starved for 16 h, incubated for 1 h with 10 μM VPC03090-P or vehicle in serum-free medium containing 0.1% fatty acid-free bovine serum, and stimulated where indicated for 5 min with either 100 nM S1P or 1 μM SEW2871. The cells were then detached with a scraper, harvested in ice-cold phosphate-buffered saline (PBS), collected by centrifugation, and resuspended in cell lysis buffer [50 mM Tris, pH 8.0, 125 mM NaCl, 20 mM CHAPS, 2 mM dithiothreitol, 1 mM EDTA, 2 mM sodium vanadate, 10 mM NaF, 1 mM phenylmethylsulfonyl fluoride, and protease inhibitor cocktail (Roche Diagnostics, Indianapolis, IN)]. Cells were lysed by repeated passage through a 28-gauge needle. The cell lysis homogenate was centrifuged to collect the supernatant. Protein concentration of the supernatant fluid was determined by bicinchoninic acid assay, and 128 μg of protein were loaded into each lane of a 4 to 20% SDS-polyacrylamide gel electrophoresis gel (Thermo Fisher Scientific). After electrophoresis and transfer to a nitrocellulose membrane, bound proteins were detected using the following antibodies from Cell Signaling Technology (Danvers, MA): rabbit monoclonal antibody to phospho-Akt, rabbit polyclonal antibody to phospho-p44/42 extracellular signal-regulated kinase (p-ERK1/2), rabbit monoclonal antibody to Akt, and rabbit polyclonal antibody to ERK1/2. We assessed equal protein loading using a β-actin antibody (Cell Signaling Technology). Detection was achieved using a goat anti-rabbit secondary antibody conjugated to an IRDye 800 CW infrared dye (LI-COR Biosciences, Lincoln, NE). The blot was digitally imaged in an Odyssey Infrared Imaging unit (LI-COR Biosciences), and signal intensity of the detected bands was quantified using Odyssey Imaging Software version 3.0 (LI-COR Biosciences).

Intracellular Ca^{2+} Mobilization assay. CHO cells expressing either $hS1P_2$ or $hS1P_3$ were plated in 96-well, clear-bottom, black-wall microplates (Corning Life Sciences, Lowell, MA) and grown overnight to confluence. The cells were washed with 1× PBS and loaded with the Ca^{2+} indicator Fluo-4 by incubation in a solution containing 1.8 μM Fluo-4AM ester, 4.5 mM NaOH, and 2.5 mM probenecid in a loading buffer of Hanks' balanced salt solution, initial pH 6.4, containing 20 mM HEPES and 0.1% fatty acid-free bovine serum albumin. After incubation in this solution for 30 min at 37°C, the cell monolayers were washed three times with PBS, and Hanks' balanced salt solution was added. Ca^{2+} signals were measured as a function of fluorescence in response to compound addition within a FLEXStation (Molecular Devices, Sunnyvale, CA).

Liquid Chromatography-Mass Spectrometry Quantification. Biological samples were extracted using a protocol modified from that of Shaner et al. (2009). Plasma samples (100 μl) were added to glass vials containing 1 ml of 3:1 methanol/chloroform solution. After addition of 2 μl of an internal standard solution containing 20 μM 1-(hydroxymethyl)-3-(3-nonaphenyl)cyclobutane (VPC03099) (a C9 analog of VPC03090) and 2 μM 3-(3-heptylphenyl)-1-(phosphonooxymethyl)cyclobutane (VPC03093) (a C7 analog of VPC03090-P), the samples were vortexed and then sonicated for 10 min in a water-bath sonicator. The samples were incubated overnight at 48°C, allowed to cool, and then supplemented with 100 μl of 1 M potassium hydroxide in methanol, followed by vortexing and sonication for 10 min. After a 2-h incubation at 37°C, 10 μl of glacial acetic acid was added, and then the samples were transferred to Eppendorf tubes and centrifuged at 10,000*g* for 10 min at 4°C. The supernatant was transferred to glass vials and dried under a nitrogen stream. Dried samples were then resuspended in 200 μl of liquid chromatography-mass spectrometry (LC-MS)-grade methanol, vortexed, and centrifuged in Eppendorf tubes at 12,000*g* for 12 min at 4°C. Forty-microliter samples of the supernatant were analyzed by LC-MS using a Shimadzu UFLC High-Performance Liquid Chromatograph (Shimadzu Scientific Instruments, Columbia, MD) equipped with an EC 125/2 Nucleodur C8 Gravity 5-μm column (125 mm, 2 mm) (Macherey-Nagel, Bethlehem, PA) connected to an ABI 4000 QTrap triple quadrupole mass spectrometer (Applied Biosystems, Foster City, CA). Chromatography was carried out at room temperature using 10% methanol, 90% water as solvent A, and 90% methanol, 10% water as solvent B. Both solvents were supplemented with 0.1% formic acid and 5 mM ammonium formate. Total flow was 0.33 ml/min. and the following gradient was used: 100% solvent A for 1 min, a linear gradient from 85% solvent B to 100% solvent B in 6 min, and 100% solvent B for 2 min. Retention times were between 5 and 6 min. Analyte detection was carried out using the following transitions in positive mode under optimal voltages for each analyte: 290.2 → 255.2 and 290.2 → 143.0 (VPC03090); 370.2 → 272.2 and 370.2 → 82.0 (VPC03090-P); 304.3 → 143.1 and 304.3 → 157.1 (VPC03099, C9 analog of VPC03090); 356.2 → 258.1 and 356.2 → 82.0 (VPC03093, C7 analog of VPC03090-P). The mass spectrometry parameters were as follows: curtain gas, 20; collision gas, medium; ionspray voltage, 5500; temperature, 550; ion source gas 1, 10; ion source gas 2, 0; declustering potential, 76; entrance potential, 10. Peak areas for analytes VPC03090 and VPC03090-P were determined based on integration of peak areas and corrected for recovery using the internal standards. Molar concentration of the analytes in biological samples was obtained from a standard curve. A standard curve was run for each experiment.

Lymphopenia Assessment. Mice were dosed with compound (as indicated in the figures) dissolved in water containing 2% hydroxypropyl β-cyclodextrin (Cargill, Inc., Cedar Rapids, IA). Blood was collected from the orbital sinus of lightly anesthetized mice. Periph-

eral lymphocytes were counted using a Hemavet 950 blood analysis unit (Drew Scientific, Oxford, CT) calibrated for mouse blood.

4T1 Mouse Mammary Cancer Model. Mouse 4T1 breast cancer cell lines (syngeneic on BALB/c genetic background) were obtained from the American Type Culture Collection and cultured in complete Dulbecco's modified Eagle's medium (Invitrogen), 10% (v/v) fetal bovine serum (Perbio Science UK Ltd., Chester, Cheshire, UK), and 1% penicillin/streptomycin (Invitrogen), at 37°C in a 5% CO_2, 95% air atmosphere. Tumor fat pad experiments were performed by injecting 4T1 cells (10^5 in 10 μl of PBS) injected into the fat pad of the fourth mammary gland of female BALB/c mice of 6 weeks of age (Charles River Breeding Laboratories, Portage, MI) as described previously(David et al., 2010). Animals were treated from day 1 until day 14 with VPC03090 (6.2 mg/kg/day) by intraperitoneal injection. Fourteen days after tumor cell injection, animals were sacrificed and primary tumors were collected. Tumor volumes were determined using a Vernier caliper. Tumor volume (TV; expressed in mm^3) was calculated using the following equation: TV = (length × width^2)/2.

Statistical Analysis. Binding curve and concentration-response data were analyzed by nonlinear regression with a sigmoidal dose-response fit model in Prism software to yield IC_{50} or EC_{50} values and their associated 95% confidence intervals. Peripheral lymphocyte count data were analyzed in Prism where indicated by Student's two-tailed *t* test or one-way analysis of variance (ANOVA) as appropriate. Additional details on statistical analysis can be found in the figure legends.

Results

Effect of VPC03090-P on S1P Receptor Activity. Through an investigation into the chemical space surrounding the sphingosine analog FTY720 (Fig. 1), we generated a conformationally constrained analogous compound in which the aryl substituent of FTY720 was changed from *para* to *meta*, and the ethyl linker was modified to a cyclobutyl ring. We designated this compound VPC03090 (Fig. 1). The phosphorylated form of VPC03090 (VPC03090-P) was also synthesized (Fig. 1), as were alcohol and phosphorylated species of analogs where the length of the alkyl hydrocarbon group ranged from 7 to 10 carbon atoms.

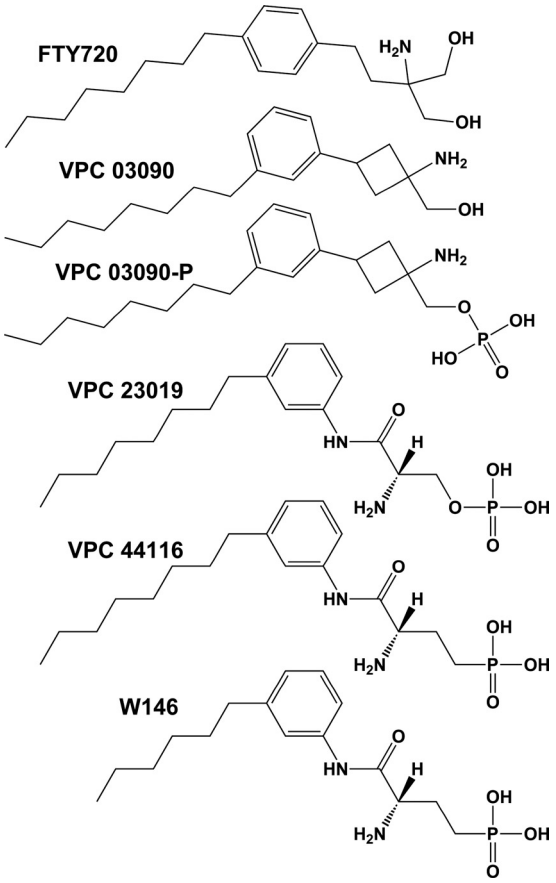

Fig. 1. Chemical structures of FTY720 and analogous compounds.

The effect of VPC03090-P on all five S1P receptor subtypes was assessed in a GTP[γ-^{35}S] binding assay as shown in Table 1. We observed inverse agonism with $hS1P_1$ and $hS1P_3$ receptors suggesting antagonism by VPC03090-P at these receptors. VPC03090-P produced concentration-dependent, parallel rightward shifts in the S1P agonist concentration-effect curve at human $S1P_1$ (Fig. 2A), mouse $S1P_1$ (Fig. 2B), and human $S1P_3$ (Fig. 2C), which is consistent with the compound being a competitive antagonist. Analysis of EC_{50} best-fit and confidence interval linear regression data found that for $hS1P_1$ and $hS1P_3$ 100 nM VPC03090-P evoked a significant shift in S1P potency at the receptor. Treatment with 1 μM VPC03090-P significantly shifted the EC_{50} value of S1P by one log order at $hS1P_1$, $mS1P_1$, and $hS1P_3$.

We determined VPC03090-P antagonism to be $S1P_{1/3}$-selective through the results obtained from the other S1P receptors. VPC03090-P demonstrated agonist activity at $hS1P_4$ and $hS1P_5$. Specifically, VPC03090-P was more potent and efficacious than S1P at $hS1P_4$ (Supplemental Fig. 1A). The EC_{50} values for S1P and VPC03090-P (56 and 17.7 nM, respectively) were significantly different, and the E_{max} of VPC03090-P relative to S1P was 1.7. At $hS1P_5$, VPC03090-P was equally potent but less efficacious than S1P (Supplemental Fig. 1B). Respective EC_{50} values of 4.4 and 2.4 nM for S1P and VPC03090-P were not significantly different. The E_{max} of VPC03090-P relative to S1P was 0.26. VPC03090-P exhibited neither agonism nor antagonism at $hS1P_2$ in a Ca^{2+} mobilization assay. The presence of the phosphate group seemed necessary for activity at $S1P_{1/3/4/5}$, because VPC03090 (the nonphosphorylated form) lacked significant activity at these receptors for concentrations up to 10 μM in the GTP[γ-^{35}S] binding assay (data not shown). To determine receptor specificity further, we screened VPC03090-P at members of a closely related family of receptors, the lysophosphatidic acid (LPA) receptors. VPC03090-P was devoid of activity at LPA1 and LPA3 at concentrations up to 10 μM in the GTP[γ-^{35}S] binding assay (data not shown).

Affinity of VPC03090-P for S1P Receptors. Dose ratios were determined from shifts in S1P EC_{50} values produced by VPC03090-P antagonism at receptors $S1P_1$ and $S1P_3$ in the GTP[γ-^{35}S] binding assay (Fig. 2). A Schild regression analysis of these data yielded the following K_i values: 24 nM ($hS1P_1$), 14 nM ($mS1P_1$), and 51 nM ($S1P_3$). As an independent test of these affinity measurements, a whole-cell radioligand binding assay was performed using CHO cells overexpressing each particular S1P receptor subtype. Binding was measured as the amount of tracer S1[^{33}P] bound to the cells in the absence or presence of competitor, either nonradiolabeled S1P or VPC03090-P. The K_i or K_d value was determined using the Cheng-Prusoff equation, and the IC_{50} values were obtained from the radioligand binding displacement curves. The VPC03090-P affinity constant values obtained by radioligand binding studies closely mirror EC_{50} values de-

TABLE 1

Characterization of VPC03090-P as a ligand for the different subtypes of the S1P receptor.

VPC03090-P binding parameters for recombinant $mS1P_1$ and $hS1P_{1-5}$ receptors. Activity of VPC03090-P at the S1P receptor was determined from a GTP[γ-^{35}S] binding assay carried out using membranes prepared from CHO cells expressing each of the S1P receptor subtypes separately (except $S1P_2$). Elevated levels of bound GTP[γ-^{35}S] in response to increasing VPC03090-P concentrations were designated as agonist activity, whereas a rightward shift in the concentration-response curve of S1P upon coapplication of VPC03090-P at a fixed concentration was designated as antagonist activity. EC_{50} values were determined by nonlinear regression analysis from a sigmoidal dose-response curve fit of VPC03090-P concentration-response data. In the case of antagonism, K_i values were obtained by Schild Regression analysis of GTP[γ-^{35}S] assay data as described under *Materials and Methods*. Affinity values (K_i or K_d) were independently determined from the Cheng-Prusoff calculation using IC_{50} values obtained in a radioligand binding assay as detailed under *Materials and Method*. $S1P_2$ receptor activity in response to VPC03090-P was evaluated using a Ca^{2+} mobilization assay.

S1P Receptor	VPC03090-P Activity	EC_{50}	E_{max} Relative to S1P	K_i from Schild Regression	K_i from Radioligand Binding	K_d from Radioligand Binding
		nM			*nM*	
$mS1P_1$	Antagonist	N.A.	N.A.	14	21.3	N.A.
$hS1P_1$	Antagonist	N.A.	N.A.	24	21	N.A.
$hS1P_2$	No activity	N.A.	N.A.	N.A.	N.A.	N.A.
$hS1P_3$	Antagonist	N.A.	N.A.	51	58.7	N.A.
$hS1P_4$	Agonist	17.7	1.7	N.A.	N.A.	17.3
$hS1P_5$	Partial agonist	2.4	0.26	N.A.	N.A.	2.3

N.A., not applicable.

rived from GTP[γ-^{35}S] agonist concentration-response curves ($hS1P_4$ and $hS1P_5$) or Schild regression analysis of competitive antagonism ($S1P_1$ and $S1P_3$) (Table 1). Our results document that the affinity of VPC03090-P for these S1P receptors lies in the range of the receptors' affinity for the natural ligand, S1P (Anliker and Chun, 2004), and VPC03090-P displayed highest affinity for $S1P_5$, followed by $S1P_4$, $S1P_1$, and $S1P_3$ (Table 1).

We next compared the potency of VPC03090-P to that of other S1P receptor antagonists by examining the 95% confidence intervals for the EC_{50} value of S1P in the presence of 1 μM antagonist. VPC03090-P was indistinguishable in potency compared with VPC44116 (Fig. 1) at $S1P_1$, whereas at $S1P_3$, VPC03090-P was significantly more potent than (*R*)-phosphoric acid mono-[2-amino-2-(3-octyl-phenylcarbamoyl)-ethyl] ester (VPC23019) (Fig. 1), VPC44116, and W146 (Fig. 1) (data not shown). Comparison of S1P receptor antagonist affinities at all of the S1P receptors is provided in Supplemental Table 1.

Influence of VPC03090-P on S1P Receptor Signaling. Next, we investigated whether VPC03090-P behaves as an antagonist of S1P receptor function. Prompted by previous observations that $S1P_1$ signaling promotes downstream enhancement of phosphatidylinositol 3-kinase activity and phosphorylation of Akt and ERK (Pyne and Pyne, 2000; Ishii et al., 2004) and the $S1P_1$-selective antagonist W146 inhibits S1P- or SEW2871-induced phosphorylation of Akt and ERK in CHO cells expressing $hS1P_1$ (Sanna et al., 2006), we determined the effect of VPC03090-P on ERK1/2 phosphorylation. Using a whole-cell assay consisting of CHO cells expressing $hS1P_1$, we found that both S1P and SEW2871 induced significant phosphorylation of ERK1/2 in the presence of vehicle, yet this ERK1/2 phosphorylation was significantly inhibited in the presence of VPC03090-P (Fig. 3, A and B). We observed a similar trend in S1P- or SEW2871-evoked Akt phosphorylation, which was also inhibited in the presence of VPC03090-P (not shown). No significant difference was found between levels of ERK1/2 phosphorylation in the presence of vehicle alone versus VPC03090-P alone.

We examined the effect of VPC03090-P on $S1P_3$ receptor function by taking advantage of the fact that the $S1P_3$ receptor couples to G_q to influence inositol triphosphate formation and mobilization of Ca^{2+} from intracellular stores (Ishii et al., 2004). Specifically, we investigated changes in intracellular Ca^{2+} in CHO cells expressing the $S1P_3$ receptor. We found that VPC03090-P significantly decreased the potency of S1P as a promoter of intracellular Ca^{2+} mobilization (Fig. 3C). Addition of 1 μM VPC03090-P significantly shifted the EC_{50} value for S1P in this assay by more than one log order. VPC03090-P alone produced no change in intracellular Ca^{2+} signal in agreement with the lack of positive efficacy of VPC03090-P at the $S1P_3$ receptor observed in our broken cell assays.

Pharmacokinetic Parameters of VPC03090 in Mice. The structural similarity between VPC03090 and FTY720 (Fig. 1) suggested that VPC03090 could also be a substrate for sphingosine kinases. Accordingly, in vitro testing with recombinant sphingosine kinases revealed that VPC03090 was a substrate for both human and mouse sphingosine kinase 2 (K_m ~23 μM) but not sphingosine kinase 1 (Yugesh Kharel and Kevin Lynch, unpublished observations). These observations prompted us to establish a quantitative LC-MS method for measuring levels of VPC03090 and VPC03090-P in plasma from mice that were administered VPC03090. Plasma levels in mice 16 h after a single 10 mg/kg i.p. dose of VPC03090 were as follows: 860 nM ($\pm$ 142 nM) VPC03090-P and 568 nM ($\pm$ 79.7 nM) VPC03090 ($n = 5$). We next assessed oral availability and duration of VPC03090 in mice after a single dose of VPC03090 (10 mg/kg) delivered by oral gavage. Our results demonstrate that VPC03090 is rapidly phosphorylated in vivo. As Fig. 4 illustrates, VPC03090-P appears in plasma within 30 min (our earliest time point). The approximate phosphorylated/alcohol species ratio of 1:1 that was found at 30 min persisted for 6 days after a single dose (Fig. 4), revealing an in vivo interconversion between VPC03090 and VPC03090-P. Using an exponential decay model, we determined the half-life of VPC03090-P in these mice to be 30 h.

To ascertain which sphingosine kinase is responsible for the phosphorylation of VPC03090 in vivo, we treated sphingosine kinase 2 null mice with VPC03090 (30 mg/kg i.p.) and analyzed plasma samples obtained 15 h after dosing. In this case, we found that plasma VPC03090 concentrations were in the micromolar range, but we failed to detect VPC03090-P, indicating that VPC03090-P was either absent or existed at concentrations below the limit of detection of our LC-MS method (approximately 2.5 nM) (data not shown; $n = 4$). We were also unable to detect VPC03090-P in plasma at longer time points, 2 and 4 days, after a single 10 mg/kg i.p. dose of VPC03090 (data not shown). These experiments demonstrate

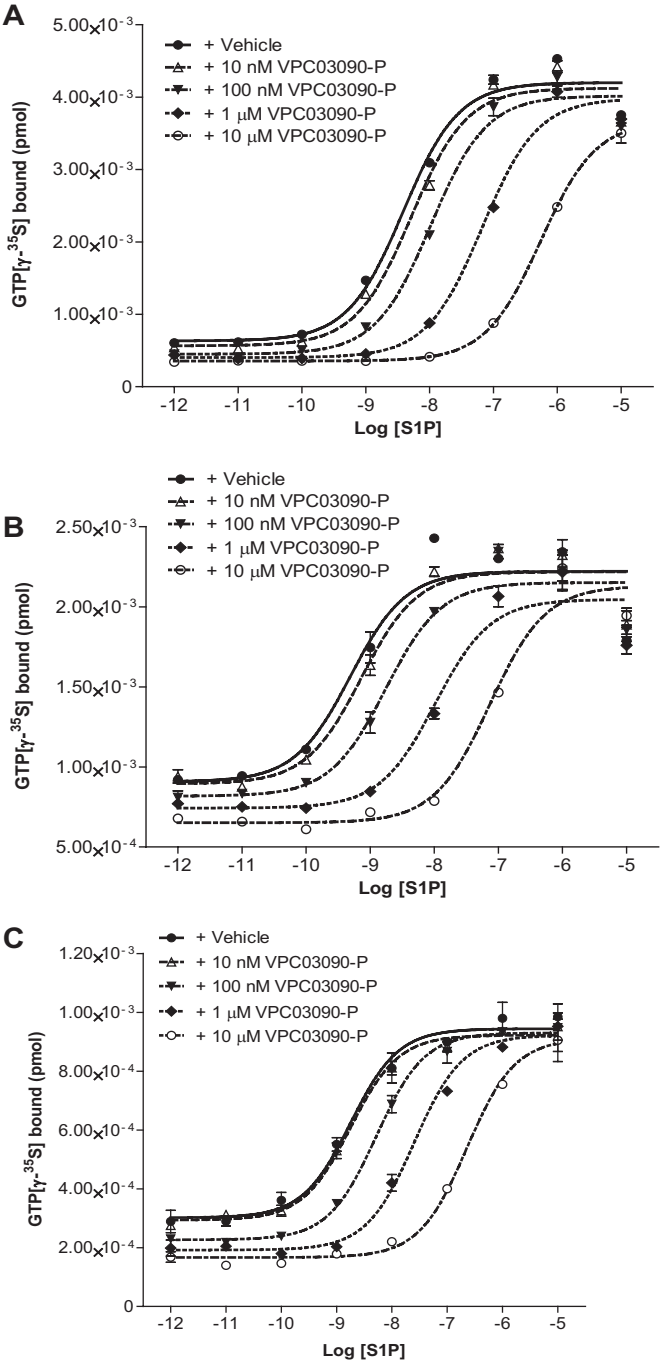

Fig. 2. Effect of VPC03090-P on S1P receptor activity in vitro. Data shown correspond to the results of a GTP[γ-^{35}S] binding assay carried out using membranes from CHO cells expressing a particular S1P receptor. The amount of GTP[γ-^{35}S] bound to the membranes under the conditions described in the figure (S1P concentration range + vehicle or VPC03090-P) is represented in units of pmol. Each data point reflects the average of a duplicate with error bars illustrating the S.E.M. A, competitive antagonism of VPC03090-P for the hS1P$_1$ receptor. Dose ratios were calculated from these curves, and Schild regression yielded a K_i value of 24 nM for VPC03090-P at hS1P$_1$. B, competitive antagonism of VPC03090-P for the mS1P$_1$ receptor. Dose ratios were calculated from these curves, and Schild regression produced a K_i value of 14 nM for VPC03090-P at mS1P$_1$. C, competitive antagonism of VPC03090-P for the hS1P$_3$ receptor. Dose ratios were calculated from these curves, and Schild regression produced a K_i value of 51 nM for VPC03090-P at hS1P$_3$.

that in vivo phosphorylation of VPC03090 occurs mostly, if not exclusively, via sphingosine kinase 2. Unfortunately, we were unable to test this hypothesis using higher doses of VPC03090 because VPC03090 was found to be lethal at doses more than 30 mg/kg i.p. We also found that the lethal dose of VPC03090 for sphingosine kinase 2 null mice is approximately similar to that for wild-type animals of the same genetic background. This suggests that the alcohol form is responsible for this effect because according to our measurements sphingosine kinase 2 null mice are unable to phosphorylate VPC03090.

Modulation of S1P$_1$ Activity In Vitro and In Vivo by Alteration of Alkyl Chain Length. We synthesized VPC03090-P analogs in which the alkyl chain was seven (C7), nine (C9), or 10 (C10) carbon atoms to analyze the SAR for this part of the VPC03090-P molecule. In vitro analysis of activity at the S1P$_1$ receptor revealed EC$_{50}$ values of 10, 30, and 178 nM for S1P, C10-P analog, and C9-P analog, respectively. Moreover, the VPC03090-P analogs exhibited different efficacy at S1P$_1$. The seven-carbon (C7) and eight-carbon (C8) hydrocarbon chain analogs showed negative or neutral efficacy, whereas installation of the C9 chain presented positive efficacy/agonism that was exaggerated in the C10 analog (Fig. 5A). The E_{max} values (relative to S1P) for the C9 and C10 compounds were 0.09 and 0.27, respectively. This trend of increasing efficacy at S1P$_1$ with increased alkyl chain length had been previously observed for our original S1P receptor antagonist series of alkyl phenyl amide compounds that included VPC23019 (Davis et al., 2005).

A well established biomarker of S1P$_1$ agonism is lymphopenia, a reduction of peripheral lymphocytes resulting from their sequestration in secondary lymphoid organs (Brinkmann et al., 2002; Mandala et al., 2002; Forrest et al., 2004; Sanna et al., 2004). In agreement with our in vitro analysis of phosphorylated analog efficacy at S1P$_1$, the C10 analog of VPC03090 significantly lowered peripheral lymphocyte counts in mice (Fig. 5B), indicating that this analog is also a prodrug, presumably activated by sphingosine kinase 2, as is the case for VPC03090 and FTY720. Although slight positive efficacy was observed in the GTP[γ-^{35}S] assay for the C9 analog, no significant lymphopenia was evoked by this compound at 16 h after a 10 mg/kg i.p dose (data not shown). This suggests that the lymphopenia only occurs above a threshold of positive agonism at the S1P$_1$ receptor that lies somewhere between that of the C9 and C10 analogs. The C8 compound VPC03090 produced no significant changes in peripheral lymphocyte counts over a dose range of 1 to 15 mg/kg i.p. in mice (Fig. 5C). In these same mice, VPC03090-P levels increased with dose escalation of VPC03090, and the VPC03090-P concentration achieved in plasma was well above the K_i value (21 nM) for the S1P$_1$ receptor (data not shown).

No significant inhibition of SEW2871-induced lymphopenia was produced by coadministration of VPC03090 in wild-type mice (data not shown). We sought to effectively rule out any potential interference in vivo from VPC03090-P-induced S1P$_4$ agonism in our attempt to observe inhibition of lymphopenia. We performed the lymphopenia assay in mice null for S1P$_4$ and found that (similar to results in wild-type mice) VPC03090 neither induced lymphopenia alone, nor reversed

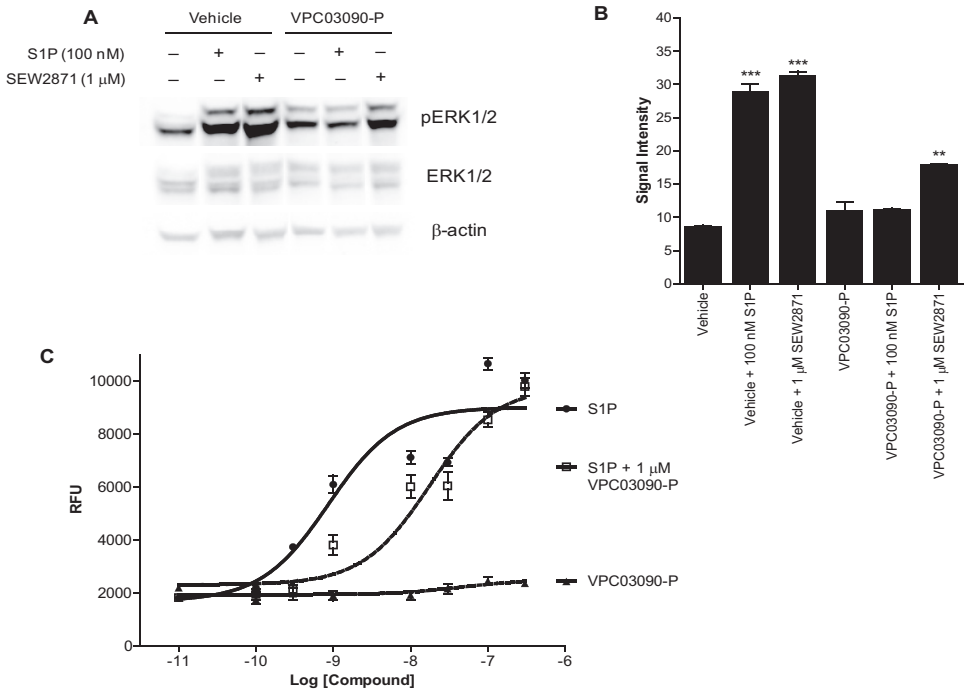

Fig. 3. Inhibition of signaling targets downstream of S1P receptors. A, Western blot to detect phosphorylation state of ERK1/2 in CHO cells expressing human $S1P_1$. Cells were serum-starved for 16 h, then incubated with 10 μM VPC03090-P or vehicle for 1 h, and then stimulated where indicated by 100 nM S1P or 1 μM SEW2871 for 5 min. A standardized protein amount of 128 μg was loaded in all lanes. The experiment was performed in duplicate for all conditions with representative results shown here. B, quantification of signal intensity for pERK1/2 bands detected on Western blot. Signal intensity of phosphorylated ERK1/2 protein bands detected by infrared imaging as described under *Materials and Methods* was quantified using Odyssey Infrared Imaging software (LI-COR, Inc.) and presented here in arbitrary units. Each column bar represents the average of a duplicate, and error bars depict the S.E.M. Results were analyzed for statistical significance within Prism software by performing a one-way ANOVA test, followed by a Newman-Keuls multiple comparison post-test. **, $p < 0.01$ for VPC03090-P + 100 nM S1P versus VPC03090-P + 1 μM SEW2871 comparison. ***, $p < 0.001$ for vehicle + 100 nM S1P versus vehicle comparison, and separately, vehicle + 1 μM SEW2871 versus vehicle comparison. C, results from a Ca^{2+} mobilization assay using CHO cells expressing human $S1P_3$. Relative fluorescence units (RFU) indicate the amount of fluorescence produced from a Ca^{2+}-sensing fluorophore in response to a concentration range of applied S1P, VPC03090-P, or coapplication of S1P and a fixed concentration of VPC03090-P. Each data point represents the average of a quadruplicate, with the error bars indicating the S.E.M..

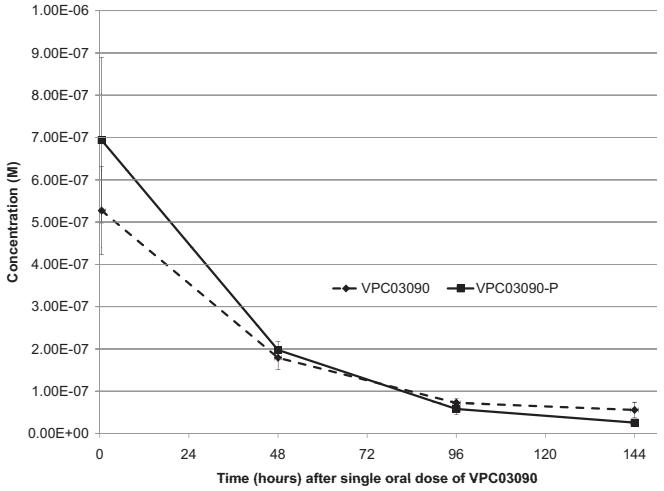

Fig. 4. Quantification of VPC03090 and VPC03090-P levels from mouse plasma over time after an oral dose of VPC03090. Data points shown depict the average concentrations (molarity) of VPC03090 (♦, dashed line) and VPC03090-P (■, solid line) in mouse plasma at 30 min (0.5 h), 2 days (48 h), 4 days (96 h), and 6 days (144 h) after a single oral dose (10 mg/kg) of VPC03090 to wild-type C57BL/6 mice. Error bars represent S.D. ($n = 5$ for all points except $n = 4$ for 144-h time point). Quantification of VPC03090 and VPC03090-P was performed by LC-MS as described under *Materials and Methods*.

the lymphopenia evoked by the $S1P_1$-selective agonist SEW2871 (Supplemental Fig. 2A). Thus, activation of $S1P_4$ does not seem to be contributing to the lack of detectable VPC03090 antagonism of $S1P_1$ influence over lymphocyte trafficking.

Assessment of Effects on Mouse Lung Endothelial Vascular Integrity. Alkyl phenyl amide phosphonate $S1P_1$ antagonists have been shown to compromise vascular integrity of mouse lung endothelium, leading to extravasation of Evans blue dye into lung tissue (Sanna et al., 2006; Foss, et al., 2007). We therefore tested whether VPC03090, which is based on a different chemical scaffold, would produce a similar effect and provide support to the contention that $S1P_1$ antagonism adversely affects the integrity of endothelial barriers. However, we were unable to induce any significant vascular leakage by the use of VPC03090 or VPC03090-P, despite having tested various doses, routes of administration, and exposure times (data not shown).

These negative results prompted us to test the hypothesis that the lack of VPC03090- (or VPC03090-P)-evoked vascular leakage was perhaps caused by the opposing effects of potent $S1P_1$ and $S1P_3$ receptor antagonism. For example, the $S1P_3$-$G_{12/13}$-Rho signaling pathway is seen as a counterbalance to the protective effects of $S1P_1$-$G_{i/o}$-Rac signaling in the modulation of vascular integrity (Brinkmann, 2007). Whereas RNA interference-mediated silencing of $S1P_1$ (or Rac) prevents vascular barrier reinforcement, silencing of $S1P_3$ (or Rho) prevents barrier disturbance (Brinkmann, 2007). We compared VPC44116 and VPC03090-P for effects of vascular leakage at the same dose and route of administration in $S1P_3$

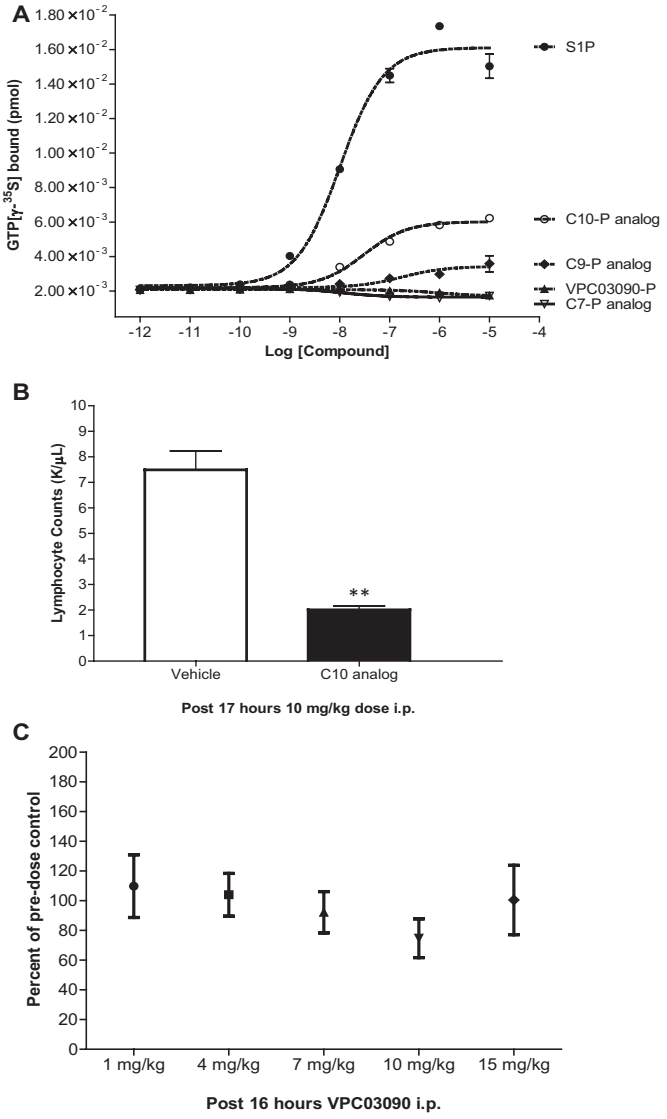

Fig. 5. Influence of alkyl chain length on efficacy at $S1P_1$ both in vitro and in vivo. A, results from a GTP[γ-^{35}S] assay using VPC03090-P analogs with alkyl chain lengths ranging from 7 to 10 carbon atoms. Membrane fractions from CHO cells expressing human $S1P_1$ were used in this assay. The amount of GTP[γ-^{35}S] bound to the membranes after incubation with the designated compound is depicted in units of pmol. Data points reflect the average of a duplicate with error bars representing the S.E.M. B, effect of C10 analog of VPC03090 on peripheral lymphocyte counts in mice. Results shown are peripheral lymphocyte counts taken from mouse blood samples 17 h after a single intraperitoneal dose (10 mg/kg) of C10 analog of VPC03090 or vehicle (2% hydroxypropyl β-cyclodextrin). Error bars reflect the S.E.M. (n = 3 per group). **, p = 0.0019, C10 analog versus vehicle, Student's two-tailed t test. C, peripheral lymphocyte counts in mice in response to increasing doses of VPC03090. Results shown are peripheral lymphocyte counts obtained from mouse blood samples and expressed as percentage of predose control lymphocyte counts for the following treatment groups: 1, 4, 7, 10, and 15 mg/kg i.p. doses of VPC03090. Final lymphocyte counts were taken 16 h after dosing with VPC03090 and a cumulative 91 h after predose control sampling. Each data point represents the average percentage of predose control lymphocyte counts for that treatment group with error bars reflecting the S.E.M. (n = 5 for each group except n = 4 for 7 and 15 mg/kg treatment groups). No significant difference was found among the means of these treatment groups by one-way ANOVA.

null mice. Whereas VPC44116 produced significant vascular leakage in these *S1pr3*(−/−) mice, VPC03090-P did not (data not shown). We further considered the possibility that perhaps agonism at $S1P_4$ evoked by VPC03090-P in vivo might interfere with the manifestation of vascular leakage. To test this hypothesis, we used $S1P_4$ null mice that are devoid of this particular receptor. In the $S1P_4$ null mice, VPC44116 evoked significant extravasation of EBD into lung tissue compared with treatment with either vehicle or VPC03090-P (Supplemental Fig. 2B). As had been previously observed in wild-type and $S1P_3$ null mice, VPC03090-P did not induce any significant vascular leakage compared with vehicle in the $S1P_4$ null mice (Supplemental Fig. 2B). These data effectively rule out the possibility of prevention of vascular leakage by VPC03090-P agonism at $S1P_4$.

Impact of VPC03090 on Tumor Growth. Given the prosurvival, promigratory, and mitogenic effects of S1P, we hypothesized a possible beneficial effect of VPC03090 in pathological conditions where hyperproliferation plays a central role. To this end, we tested the antitumor efficacy of this molecule in two aggressive, immunocompetent mouse cancer models: Lewis lung carcinoma and 4T1 mammary carcinoma.

For the Lewis lung carcinoma model, we devised a dosing scheme that would sustain drug levels equivalent to an average dose of 10 mg/kg p.o. daily over the duration of the tumor model. This dosing scheme consisted of an initial loading dose of 13 mg/kg p.o., followed by a maintenance dose of 5.5 mg/kg p.o. every 24 h. The maintenance value was meant to compensate for the daily loss calculated using the half-life obtained in the experiment shown in Fig. 4. We chose 10 mg/kg p.o. as a daily dose because it is apparently well tolerated and provides VPC03090-P drug levels of more than 10-fold the K_i at the $S1P_1$ receptor (Fig. 4 and Table 1). The described dosing regimen was initiated once syngeneic subcutaneous Lewis lung carcinoma tumors had became palpable in the flank of C57BL/6 mice. An analysis of tumor volume over 2 weeks of daily treatment found that VPC03090 did not significantly inhibit tumor growth in this model (data not shown).

In the 4T1 mammary cancer model, a dosing scheme of 6.2 mg/kg/day i.p. of VPC03090 was used. VPC03090 significantly reduced tumor volume in this model. As shown in Fig. 6, median tumor volume was reduced approximately

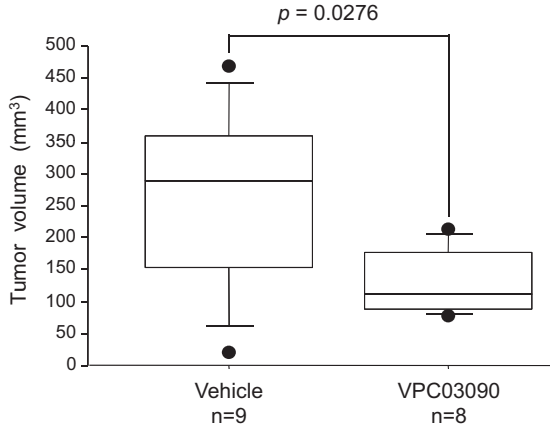

Fig. 6. Effect of VPC03090 on primary breast tumor growth in a syngeneic immunocompetent 4T1 mouse model. 4T1 cells were injected in the mammary gland of normal syngeneic female BALB/c mice. Treatment with vehicle or VPC03090 (6.2 mg/kg/day i.p.) was initiated on the day of cancer cell injection (day 1). At day 14, primary tumors were resected and measured by calipers. TV was calculated using the equation TV = (length × width^2)/2 and is represented here (in mm^3) using box plots.

3-fold by VPC03090 treatment compared with vehicle treatment.

Discussion

S1P receptor antagonists are desirable as tools to probe S1P biology and are necessary to learn whether blockade of S1P signaling at the receptor level might be a viable therapeutic strategy. Since the introduction of FTY720 (Fig. 1), a S1P receptor pan agonist prodrug now in clinical use (Brinkmann et al., 2010), numerous studies have focused on obtaining FTY720 analogs with improved potency and/or selectivity. In this study we present VPC03090, an FTY720 analog that combines selective S1P receptor antagonism with similar pharmacokinetic characteristics to FTY720. We were guided by our previous studies on the SAR of FTY720-P that yielded the first $S1P_{1/3}$ receptor antagonist, VPC23019 (Davis et al., 2005). The conformationally constrained VPC23019 (Fig. 1) proved to be short-lived in vivo, presumably because of rapid dephosphorylation (Lynch and Macdonald, 2008). Its phosphonate analog VPC44116 (Fig. 1) (Foss et al., 2007), however, persists longer in rodents ($T_{1/2}$ = 2–3 h) and a shorter chain (C6 versus C8) version, W146 (Fig. 1), has increased $S1P_1$ selectivity (Sanna et al., 2006). These molecules, which are inverse agonists in GTP[γ-^{35}S] binding assays, have double-digit nanomolar affinities for human and mouse $S1P_1$ receptors (Supplemental Table 1).

VPC03090 was built on the FTY720 scaffold, but incorporates a crucial structural feature of the VPC23019 series, installation of the alkyl group *meta* rather than *para* as in FTY720. We had found previously that conversion of the phenyl ethyl moiety in FTY720 to phenyl cyclopentyl resulted in a long-lived, orally available S1P prodrug that was an $S1P_1$ agonist and $S1P_3$ antagonist (1-[1-amino-3-(4-octylphenyl)cyclopentyl]methanol; VPC01091) (Zhu et al., 2007). Thus our strategy to avoid another essential feature of the VPC23019 molecule, i.e., the requirement of *s* configuration of the amino carbon (which precludes recycling of the alcohol species by rephosphorylation as in FTY720), was solved by conversion of the phenyl ethyl "linker" in FTY720 to phenyl cyclobutyl. The resulting amino alcohol, VPC03090, combines the dual $S1P_{1/3}$ antagonist (and $S1P_{4/5}$ agonist) properties of the lead antagonist VPC23019 with the prodrug/active drug (alcohol/phosphate) cycling of FTY720 and thereby captures the oral availability and in vivo longevity of the latter compound.

We anticipate that VPC03090 can be used to investigate the in vivo consequences of long-term $S1P_{1/3}$ antagonism. Pharmacodynamic studies of the shorter-lived antagonists VPC44116 and W146 in mice have yielded two salient results. First, they do not induce lymphopenia (Sanna et al., 2006; Foss et al., 2007) in discrepancy with the proposed "functional antagonist" mechanism of $S1P_1$ agonist-driven lymphopenia (Matloubian et al., 2004). Second, they induce pulmonary vascular leakage (Sanna et al., 2006; Foss et al., 2007), which supports the notion that circulating S1P (Hammad et al., 2010) tonically supports endothelial barrier function via $S1P_1$ receptor activation (Marsolais and Rosen, 2009). When we administered VPC03090 to mice, we observed neither changes in circulating lymphocyte counts nor leakage of Evans blue dye.

An explanation proffered for failure of $S1P_1$ antagonists to drive lymphopenia is that these molecules are not potent enough (Pappu et al., 2007). VPC03090-P, which is nearly equipotent to other S1P antagonists at $S1P_1$ (Supplemental Table 1), might also be insufficient in this regard, even though the trough plasma levels were well into the triple-digit nanomolar range. The failure of VPC03090 to block lymphopenia driven by the $S1P_1$-selective agonist, SEW2871, supports this argument. We also considered the explanation that VPC03090-P might be highly bound to plasma proteins and thus the concentration available to the $S1P_1$ receptor would be correspondingly low. However, this thinking is belied by the lymphopenia observed in response to the equipotent $S1P_1$ agonist C10 analog of VPC03090, which would seem to be no less protein bound than the C8 VPC03090. We observed neither lymphopenia nor lymphopenia inhibition from VPC03090 in $S1P_4$ null mice, excluding any potential confounding effect from agonism at this receptor.

The lack of vascular leakage in response to VPC03090-P seems more curious. Although we have never failed to observe pulmonary leakage of Evans blue dye in response to VPC44116 in mice (2–20 mg/kg i.v. or i.p.; $n > 20$), we have not observed it in any VPC03090 (10 mg/kg i.p.)- or VPC03090-P (10 mg/kg i.p.; 2 mg/kg i.v.)-treated mice ($n > 12$). These VPC03090 and VPC03090-P dosing regimens produce concentrations of VPC03090-P in mouse plasma far in excess of its K_i value at mouse $S1P_1$ (21 nM). We considered that either the agonist activity of VPC03090-P at $S1P_4$ or the antagonist activity of VPC03090-P at $S1P_3$ might have counterbalanced the effects of $S1P_1$ antagonism, preventing vascular leakage. However, we did not observe vascular leakage in either $S1P_3$ null mice or $S1P_4$ null mice in response to VPC03090-P, which compels us to consider the possibility that the vascular leakage observed in mice treated with VPC44116 (or its C6 congener W146) is not a consequence of $S1P_1$ blockade, but rather an off-target effect of compounds with the phenyl amide scaffold. Unfortunately, deletion of the *S1pr1* gene is embryonically lethal, thus the genetically altered mice that would provide greater clarification of this issue are not available (Liu et al., 2000). Discovery of $S1P_1$-selective antagonists with in vivo stability and alternative scaffolds are called for in resolving the discrepancy in the vascular leakage phenomenon.

Numerous reports have suggested a pathological role for aberrant S1P metabolism and signaling in carcinogenesis (Xia et al., 2000; Akao et al., 2006; Oskouian et al., 2006; Pyne and Pyne, 2010; Watson et al., 2010). Indeed, S1P signaling through receptors stimulates potentially cancerous processes (Pyne and Pyne, 2000; Ishii et al., 2004). It has been proposed that S1P may be signaling at two sites concurrently to perpetuate tumor growth: 1) S1P receptors on the cancer cell to promote survival, proliferation, migration, and proangiogenic cytokine release, and 2) $S1P_1$ on the vascular endothelial cell to evoke local angiogenesis (Sabbadini, 2006). As evidence, an anti-S1P antibody reduced endothelial cell migration, cancer cell migration, proliferation, invasion, and tumor angiogenesis and inhibited tumor growth for several different cancer types (Visentin et al., 2006). Furthermore, $S1P_1$ has been demonstrated to participate in a positive-feedback mechanism with signal transducer and activator of transcription 3 to promote progression of cancer malignancy (Lee et al., 2010). Down-regulation of $S1P_1$

through pharmacological tools or small interfering RNA has been shown to decrease angiogenesis and tumor growth (Chae et al., 2004; LaMontagne et al., 2006). As a logical extension of published evidence, we conclude that an $S1P_1$ antagonist should also provide an advantageous dual mode of action. Even if a cancer cell exhibits reduced dependence on $S1P_1$ signaling for survival as a result of a mutation, tumor growth would still be restricted by insufficient nourishment because of the antiangiogenic effect of $S1P_1$ antagonism. Moreover, the specificity provided by an $S1P_{1/3}$ receptor antagonist might be more beneficial than a nonselective sphingosine kinase inhibitor or S1P antibody.

In view of the potency/affinity, bioavailability, and in vivo longevity of the $S1P_{1/3}$ antagonist prodrug VPC03090, we assessed its effectiveness for tumor growth inhibition in two mouse cancer models. The first was an ectopic Lewis lung carcinoma model in which treatment is initiated once tumors are detected by palpation. Measurements of subcutaneous tumor volume over time revealed no significant differences between vehicle- and VPC03090-treated animals. Unfortunately, we observed large deviations in tumor size in both groups, which would have prevented us from detecting an effect had there been one. Our second model was an orthotopic immunocompetent 4T1 mammary cancer model in which treatment begins the same day that cancer cells are injected into the mammary gland. In this setting, VPC03090 significantly reduced tumor volume. Several possibilities may account for the differences in efficacy between the tumor models. The 4T1 cells may depend more heavily on S1P signaling for survival or angiogenesis or may exhibit this dependence in earlier phases of tumor growth. Both tumor models shared a similar duration of treatment, but the 4T1 model initiated treatment at an earlier phase of carcinogenesis. We further speculate that perhaps the difference in tumor placement between the two models may have resulted in a greater delivery of systemic VPC03090 or VPC03090-P to the mammary tumor versus a subcutaneous tumor. Nevertheless, our finding warrants further investigation using VPC03090 and other drug-like S1P antagonists in additional cancer models.

The high degree of similarity between the mouse and human $S1P_1$ receptor coupled with the similar antagonism and binding affinity of VPC03090-P at both mouse and human $S1P_1$ support the possibility for translational research in the context of S1P-driven malignant neoplasia. VPC03090 is also a substrate for both mouse and human sphingosine kinase type 2. The translational potential is underscored by the history of FTY720, an S1P receptor prodrug agonist that is now a United States Food and Drug Administration-approved treatment for multiple sclerosis (Brinkmann et al., 2010). We anticipate that VPC03090 will inform future SAR studies, provide incentive for further S1P receptor antagonist discovery, and be useful in validation of the S1P receptors as drug targets. S1P receptor antagonists hold dual promise as research tools and potential therapeutic agents in the ongoing elucidation of S1P's contribution to both physiological tone and pathological conditions.

Acknowledgments

We thank Dr. Yugesh Kharel (University of Virginia, Charlottesville, VA) for determination of sphingosine kinase activity in vitro and guidance for Western blotting techniques; Dr. Andrew Morris (University of Kentucky, Lexington, KY) for technical expertise and assistance provided during the course of our establishing LC-MS instrumentation capability; Dr. Ruth Stornetta (University of Virginia) for technical expertise in performing perfusion of mouse vasculature for pulmonary vascular permeability studies; Gina Wimer (University of Virginia) for tail vein injections into mice; and Marie Burdick (University of Virginia) for guidance concerning the Lewis lung carcinoma model. VPC44116 was provided by Dr. Frank Foss Jr. (University of Texas, Arlington, TX). The plasmid encoding the C-terminal GFP-tagged human $S1P_1$ receptor was a gift from Dr. Timothy Hla (University of Connecticut, Storrs, CT). The *S1pr3*(−/−) mice were a gift from Dr. Richard Proia (National Institutes of Health/National Institute of Diabetes and Digestive and Kidney Diseases, Bethesda, MD).

Authorship Contributions

Participated in research design: Kennedy and Lynch.

Conducted experiments: Kennedy, David, and Peyruchaud.

Contributed new reagents or analytic tools: Zhu, Huang, Tomsig, Mathews, and Macdonald.

Performed data analysis: Kennedy, Tomsig, and David.

Wrote or contributed to the writing of the manuscript: Kennedy, Tomsig, and Lynch.

References

Akao Y, Banno Y, Nakagawa Y, Hasegawa N, Kim TJ, Murate T, Igarashi Y, and Nozawa Y (2006) High expression of sphingosine kinase 1 and S1P receptors in chemotherapy-resistant prostate cancer PC3 cells and their camptothecin-induced up-regulation. *Biochem Biophys Res Commun* **342:**1284–1290.

Anliker B and Chun J (2004) Lysophospholipid G protein-coupled receptors. *J Biol Chem* **279:**20555–20558.

Brinkmann V (2007) Sphingosine 1-phosphate receptors in health and disease: mechanistic insights from gene deletion studies and reverse pharmacology. *Pharmacol Ther* **115:**84–105.

Brinkmann V, Billich A, Baumruker T, Heining P, Schmouder R, Francis G, Aradhye S, and Burtin P (2010) Fingolimod (FTY720): discovery and development of an oral drug to treat multiple sclerosis. *Nat Rev Drug Discov* **9:**883–897.

Brinkmann V, Davis MD, Heise CE, Albert R, Cottens S, Hof R, Bruns C, Prieschl E, Baumruker T, Hiestand P, et al. (2002) The immune modulator FTY720 targets sphingosine 1-phosphate receptors. *J Biol Chem* **277:**21453–21457.

Chae SS, Paik JH, Furneaux H, and Hla T (2004) Requirement for sphingosine 1-phosphate receptor-1 in tumor angiogenesis demonstrated by in vivo RNA interference. *J Clin Invest* **114:**1082–1089.

Cheng Y and Prusoff WH (1973) Relationship between the inhibition constant (K1) and the concentration of inhibitor which causes 50 per cent inhibition (I50) of an enzymatic reaction. *Biochem Pharmacol* **22:**3099–3108.

Chiba K, Hoshino Y, Suzuki C, Masubuchi Y, Yanagawa Y, Ohtsuki M, Sasaki S, and Fujita T (1996) FTY720, a novel immunosuppressant possessing unique mechanisms. I. Prolongation of skin allograft survival and synergistic effect in combination with cyclosporine in rats. *Transplant Proc* **28:**1056–1059.

Cusack KP and Stoffel RH (2010) $S1P_1$ receptor agonists: Assessment of selectivity and current clinical activity. *Curr Opin Drug Discov Dev* **13:**481–488.

David M, Wannecq E, Descotes F, Jansen S, Deux B, Ribeiro J, Serre CM, Grès S, Bendriss-Vermare N, Bollen M, et al. (2010) Cancer cell expression of autotaxin controls bone metastasis formation in mouse through lysophosphatidic acid-dependent activation of osteoclasts. *PLoS One* **5:**e9741.

Davis MD, Clemens JJ, Macdonald TL, and Lynch KR (2005) Sphingosine 1-phosphate analogs as receptor antagonists. *J Biol Chem* **280:**9833–9841.

Forrest M, Sun SY, Hajdu R, Bergstrom J, Card D, Doherty G, Hale J, Keohane C, Meyers C, Milligan J, et al. (2004) Immune cell regulation and cardiovascular effects of sphingosine 1-phosphate receptor agonists in rodents are mediated via distinct receptor subtypes. *J Pharmacol Exp Ther* **309:**758–768.

Foss FW Jr, Snyder AH, Davis MD, Rouse M, Okusa MD, Lynch KR, and Macdonald TL (2007) Synthesis and biological evaluation of γ-aminophosphonates as potent, subtype-selective sphingosine 1-phosphate receptor agonists and antagonists. *Bioorg Med Chem* **15:**663–677.

Hait NC, Oskeritzian CA, Paugh SW, Milstien S, and Spiegel S (2006) Sphingosine kinases, sphingosine 1-phosphate, apoptosis and diseases. *Biochim Biophys Acta* **1758:**2016–2026.

Hammad SM, Pierce JS, Soodavar F, Smith KJ, Al Gadban MM, Rembiesa B, Klein RL, Hannun YA, Bielawski J, and Bielawska A (2010) Blood sphingolipidomics in healthy humans: impact of sample collection methodology. *J Lipid Res* **51:**3074–3087.

Institute of Laboratory Animal Resources (1996) *Guide for the Care and Use of Laboratory Animals*, 7th ed. Institute of Laboratory Animal Resources, Commission on Life Sciences, National Research Council, Washington DC.

Ishii I, Fukushima N, Ye X, and Chun J (2004) Lysophospholipid receptors: signaling and biology. *Annu Rev Biochem* **73:**321–354.

Kihara A and Igarashi Y (2008) Production and release of sphingosine 1-phosphate and the phosphorylated form of the immunomodulator FTY720. *Biochim Biophys Acta* **1781:**496–502.

Kiuchi M, Adachi K, Kohara T, Minoguchi M, Hanano T, Aoki Y, Mishina T, Arita M,

Nakao N, Ohtsuki M, et al. (2000) Synthesis and immunosuppressive activity of 2-substituted 2-aminopropane-1,3-diols and 2-aminoethanols. *J Med Chem* **43:** 2946–2961.
LaMontagne K, Littlewood-Evans A, Schnell C, O'Reilly T, Wyder L, Sanchez T, Probst B, Butler J, Wood A, Liau G, et al. (2006) Antagonism of sphingosine-1-phosphate receptors by FTY720 inhibits angiogenesis and tumor vascularization. *Cancer Res* **66:**221–231.
Lee H, Deng J, Kujawski M, Yang C, Liu Y, Herrmann A, Kortylewski M, Horne D, Somlo G, Forman S, et al. (2010) STAT3-induced S1PR1 expression is crucial for persistent STAT3 activation in tumors. *Nat Med* **16:**1421–1428.
Liu Y, Wada R, Yamashita T, Mi Y, Deng CX, Hobson JP, Rosenfeldt HM, Nava VE, Chae SS, Lee MJ, et al. (2000) Edg-1, the G protein-coupled receptor for sphingosine-1-phosphate, is essential for vascular maturation. *J Clin Invest* **106:**951–961.
Lynch KR and Macdonald TL (2008) Sphingosine 1-phosphate chemical biology. *Biochim Biophys Acta* **1781:**508–512.
Mandala S, Hajdu R, Bergstrom J, Quackenbush E, Xie J, Milligan J, Thornton R, Shei GJ, Card D, Keohane C, et al. (2002) Alteration of lymphocyte trafficking by sphingosine-1-phosphate receptor agonists. *Science* **296:**346–349.
Marsolais D and Rosen H (2009) Chemical modulators of sphingosine-1-phosphate receptors as barrier-oriented therapeutic molecules. *Nat Rev Drug Discov* **8:**297–307.
Matloubian M, Lo CG, Cinamon G, Lesneski MJ, Xu Y, Brinkmann V, Allende ML, Proia RL, and Cyster JG (2004) Lymphocyte egress from thymus and peripheral lymphoid organs is dependent on S1P receptor 1. *Nature* **427:**355–360.
Oskouian B, Sooriyakumaran P, Borowsky AD, Crans A, Dillard-Telm L, Tam YY, Bandhuvula P, and Saba JD (2006) Sphingosine-1-phosphate lyase potentiates apoptosis via p53- and p38-dependent pathways and is down-regulated in colon cancer. *Proc Natl Acad Sci USA* **103:**17384–17389.
Pappu R, Schwab SR, Cornelissen I, Pereira JP, Regard JB, Xu Y, Camerer E, Zheng YW, Huang Y, Cyster JG, et al. (2007) Promotion of lymphocyte egress into blood and lymph by distinct sources of sphingosine-1-phosphate. *Science* **316:**295–298.
Pyne NJ and Pyne S (2010) Sphingosine 1-phosphate and cancer. *Nat Rev Cancer* **10:**489–503.
Pyne S and Pyne NJ (2000) Sphingosine 1-phosphate signalling in mammalian cells. *Biochem J* **349:**385–402.
Sabbadini RA (2006) Targeting sphingosine-1-phosphate for cancer therapy. *Br J Cancer* **95:**1131–1135.
Sanchez T and Hla T (2004) Structural and functional characteristics of S1P receptors. *J Cell Biochem* **92:**913–922.
Sanna MG, Liao J, Jo E, Alfonso C, Ahn MY, Peterson MS, Webb B, Lefebvre S, Chun J, Gray N, et al. (2004) Sphingosine 1-phosphate (S1P) receptor subtypes $S1P_1$ and $S1P_3$, respectively, regulate lymphocyte recirculation and heart rate. *J Biol Chem* **279:**13839–13848.
Sanna MG, Wang SK, Gonzalez-Cabrera PJ, Don A, Marsolais D, Matheu MP, Wei SH, Parker I, Jo E, Cheng WC, et al. (2006) Enhancement of capillary leakage and restoration of lymphocyte egress by a chiral $S1P_1$ antagonist in vivo. *Nat Chem Biol* **2**:434–441.
Shaner RL, Allegood JC, Park H, Wang E, Kelly S, Haynes CA, Sullards MC, and Merrill AH Jr (2009) Quantitative analysis of sphingolipids for lipidomics using triple quadrupole and quadrupole linear ion trap mass spectrometers. *J Lipid Res* **50:**1692–1707.
Spiegel S and Milstien S (2003) Sphingosine-1-phosphate: an enigmatic signalling lipid. *Nat Rev Mol Cell Biol* **4:**397–407.
Visentin B, Vekich JA, Sibbald BJ, Cavalli AL, Moreno KM, Matteo RG, Garland WA, Lu Y, Yu S, Hall HS, et al. (2006) Validation of an anti-sphingosine-1-phosphate antibody as a potential therapeutic in reducing growth, invasion, and angiogenesis in multiple tumor lineages. *Cancer Cell* **9:**225–238.
Watson C, Long JS, Orange C, Tannahill CL, Mallon E, McGlynn LM, Pyne S, Pyne NJ, and Edwards J (2010) High expression of sphingosine 1-phosphate receptors, $S1P_1$ and $S1P_3$, sphingosine kinase 1, and extracellular signal-regulated kinase-1/2 is associated with development of tamoxifen resistance in estrogen receptor-positive breast cancer patients. *Am J Pathol* **177:**2205–2215.
Xia P, Gamble JR, Wang L, Pitson SM, Moretti PA, Wattenberg BW, D'Andrea RJ, and Vadas MA (2000) An oncogenic role of sphingosine kinase. *Curr Biol* **10:**1527–1530.
Zhu R, Snyder AH, Kharel Y, Schaffter L, Sun Q, Kennedy PC, Lynch KR, and Macdonald TL (2007) Asymmetric synthesis of conformationally constrained fingolimod analogs–discovery of an orally active sphingosine 1-phosphate receptor type-1 agonist and receptor type-3 antagonist. *J Med Chem* **50:**6428–6435.

Address correspondence to: Dr. Kevin R. Lynch, University of Virginia, 1340 Jefferson Park Avenue, P.O. Box 800735, Jordan Hall, Room 5227, Charlottesville, VA 22908-0735. E-mail: krl2z@virginia.edu